Hydrodynamic modes of superfluid helium adsorbed on Nuclepore

S. M. Cohen, R. A. Guyer, and J. Machta
Laboratory for Low Temperature Physics, University of Massachusetts, Amherst, Massachusetts 01003
(Received 26 August 1985)

A theory is presented to describe sound propagation in superfluid ^{4}He adsorbed on Nuclepore, a planar porous substrate. The theory predicts the dependence of the sound velocity on film thickness. For thin films the sound speed is lower than on an equivalent nonporous substrate while for thick films the reverse holds. The transition between these regimes occurs when the fluid in the pores capillary condenses. The predictions of the theory are in qualitative agreement with the experimental results of Hallock and co-workers.

I. INTRODUCTION

In the study of superfluid helium films it is desirable that they be formed on materials with large, well-characterized surfaces. For this reason Nuclepore[1] filters have been increasingly used in a variety of experiments on films, e.g., specific heat,[2] third sound,[3,4] and NMR.[5] Recently, Valles *et al.*[3] have made extensive measurements of third sound on Nuclepore that have revealed a rich structure. The purpose of this paper is to provide a theoretical basis for understanding these measurements.[6] In accomplishing this task we exhibit a formulation of the description of the third-sound mode that is both elegant and computationally powerful. The understanding which this formulation gives of the behavior of the third-sound mode in complex systems demonstrates the value of such measurements as a probe of the underlying physics and also as a diagnostic tool. As an example of the latter point, a third-sound measurement at low-^{4}He coverage on a highly disordered substrate may be used to measure the surface area and as such is equivalent to a BET measurement.

The outline of this paper is as follows. In Sec. II we discuss the equilibrium distribution of ^{4}He fluid on a Nuclepore filter. In Sec. III we formulate the theory of the sound velocity for a compressible ideal fluid adsorbed on a disordered substrate and apply this theory to helium on Nuclepore. Comparison with experiment and a summary are given in Sec. IV.

II. EQUILIBRIUM DISTRIBUTION OF ^{4}He ON NUCLEPORE

Nuclepore filter, shown schematically in Fig. 1, is composed of a polycarbonate plastic of thickness, l, perforated with randomly distributed pores of areal density, λ, and nearly uniform radius, R. The angle, θ, between the axis of the pore and the normal to the surface is randomly distributed in the range $0<\theta<\theta_{\max}$. To compare with the experiment of Ref. 3 we take the values of the parameters to be $l=10^{-3}$ cm, $R=10^{-5}$ cm, $\lambda=3\times10^{8}$ cm^{-2} and $\theta_{\max}=34°$.

Consider a ^{4}He film adsorbed on a single such filter in equilibrium with a film reservoir and an unsaturated vapor in a sample chamber. The unsaturated vapor pressure sets the chemical potential of the ^{4}He in the sample chamber and the film reservoir supplies the ^{4}He atoms necessary to bring the ^{4}He distribution on the Nuclepore into equilibrium with this chemical potential. We are interested in the distribution of ^{4}He fluid in the Nuclepore as the chemical potential is varied and the ^{4}He film thickness on the upper and lower surfaces, h, increases from a few atomic layers to more than 20 layers.

The distribution of ^{4}He in the pores depends on the balance between the van der Waals force and surface tension. For thin films the van der Waals attraction between the ^{4}He and the Nuclepore dominates, and we expect the ^{4}He to coat the walls of the pores with thickness, $h_p \gtrsim h$, as shown in Fig. 2(a). In equilibrium, chemical potential balance between the surfaces and the pores [points 1 and 2 of Fig. 2(a)] determines h and h_p so that

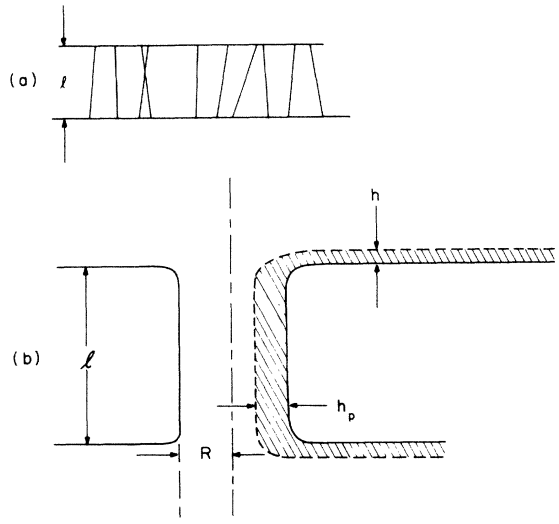

FIG. 1. Nuclepore. (a) Nuclepore filters are characterized by the areal density of pores, e.g., approximately 3×10^8 cm^2, the pore radius, $R\simeq10^{-5}$ cm, and thickness, $d\simeq10^{-3}$ cm. (b) A ^{4}He film covers the upper and lower surface of the filter to height h and the surface in the pore to height h_p. The pores, with aspect ratio $=2R/d$ of about 10^2, have angular dispersion of about 30° as suggested in (a).

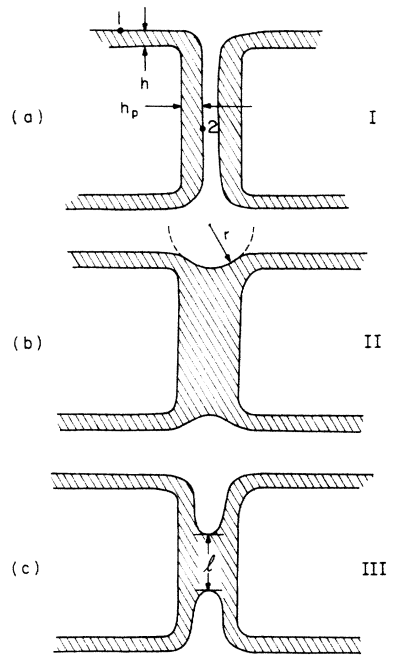

FIG. 2. Configuration. There are three configurations of the ^{4}He film. (a) Configuration I, appropriate to thin films and described by Eq. (2.1), involves chemical potential balance between point 1 and point 2 with $h_p \simeq h$ until $h \simeq 16$. (b) Configuration II, appropriate to capillary condensed pores and described by Eq. (2.2), evolves as r evolves from R to $+\infty$. (c) Configuration III, a candidate for the behavior of the film as it evolves between configuration I and configuration II, has approximately the same chemical potential as configuration II at $r=R$ independent of l, see point 3 on Fig. 3.

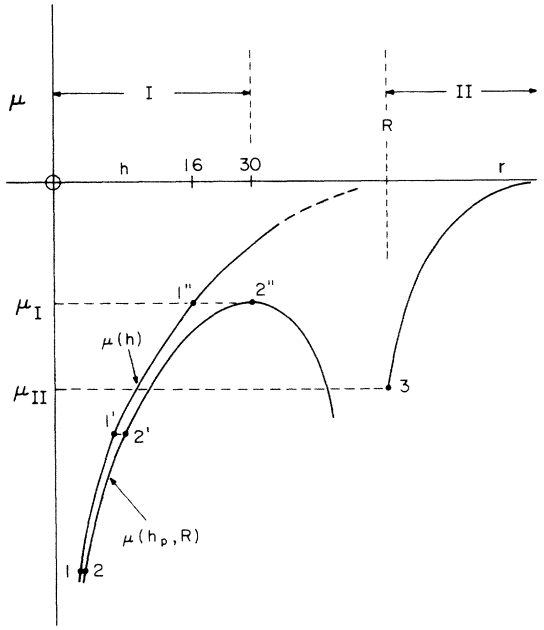

FIG. 3. Chemical potential. The chemical potential evolves as the film thickness evolves. For thin films, when configuration I is involved, h is a useful variable to describe the film; for capillary condensed films, when configuration II is involved, r is a useful variable to describe the film. Here, μ is plotted schematically as a function of h for $0 \leq h_p \leq R$, for configuration I, and as function of r for $h_p = R$, for configuration II. The amount of ^{4}He in the sample increases continuously as one goes from left to right along the horizontal axis.

$$-\alpha_v \left[\frac{a}{h}\right]^3 = \mu = -\alpha_v \left[\frac{a}{h_p}\right]^3 - \frac{\sigma}{\rho(R-h_p)} . \qquad (2.1)$$

We have taken the van der Waals potential between a ^{4}He atom and the substrate to be $V(z)=\alpha_v a^3/z^3$. ρ is the atomic density, z is the distance from the substrate measured in cm, h/a is the film thickness in layers ($\rho = a^{-3}$, $a = 3.6\times10^{-8}$ cm, $\alpha_v = 50$ K for ^{4}He on Nuclepore, and σ, the surface tension of bulk ^{4}He, is 0.31 ergs/cm^2). The second term on the right-hand side (RHS) of Eq. (2.1) comes from the change in surface energy that results from taking an atom out of the ^{4}He fluid in the pore. The content of Eq. (2.1) is illustrated in Fig. 3 in which the left-hand side (RHS) of this equation is plotted as a function of h/a (h_p/a). For very thin ^{4}He films (points 1 and 2 of Fig. 3) the van der Waals energy is much larger than the surface energy and $h \simeq h_p$.

As μ and h increase, the van der Waals energy diminishes, and equilibrium is achieved by h_p becoming increasingly larger than h. The appropriate balance is displayed as points 1' and 2' in Fig. 3. At points 1" and 2" when $\mu = \mu_I \approx 0.012$ K (the surface height is approximately 16 layers and the pore height approximately 30 layers) configuration I becomes unstable and the pores fill spontaneously. Near points 1" and 2" the fluid in the pore is elastically soft and fluctuations away from equilibrium are restored slowly, implying that the sound velocity will be very small.

The equilibrium state of the ^{4}He for relatively thick films is shown schematically in Fig. 2(b) and referred to as configuration II. Here, the pores are filled and the film profile at the ends of the pores has a radius of curvature near the central axis of the pore given by r.

Again, the equilibrium configuration is determined by chemical potential balance,

$$-\alpha \left[\frac{a}{h}\right]^3 = \mu = -\frac{2\sigma}{\rho r} . \qquad (2.2)$$

We shall not calculate here the shape of the surfaces at the ends of the pores. However, it is clear that a stable surface can exist only for $r \gtrsim R$. Thus, configuration II is a possible equilibrium state for $h \gtrsim 16$ layers and $\mu > \mu_{II} \approx -2\sigma/\rho R$. For μ slightly less than μ_{II}, equilibrium may also be achieved as shown schematically in Fig. 2(c) and referred to as configuration III. Here, the pores are partially filled with end surfaces having radii of curvature nearly independent of the filling fraction and approximately given by R. Thus, these configurations can exist only over a narrow range in chemical potential between μ_{III} and μ_{II}. Note that $\mu_I > \mu_{II} > \mu_{III}$ so that for some values of μ, more than one configuration satisfies chemical equilibrium balance.

In the range of μ for which more than one configuration is possible, the equilibrium state may be determined by minimizing the grand potential,

$$\Omega_\nu(\mu)=E_\nu(\mu)-\mu N_\nu(\mu) , \tag{2.3}$$

where ν denotes the configuration (I, II, or III), E is the total internal energy which is the sum of van der Waals, surface, and bulk contributions, and N is the total number of ^{4}He atoms. We find that for $\mu_{II}<\mu<\mu_I$, $\Omega_I<\Omega_{II}$ and when $\mu_{III}<\mu<\mu_{II}$, $\Omega_I<\Omega_{III}$. Thus as μ as increased from large negative values (thin films) the system resides in configuration I more or less until μ_I is reached at which point the pores fill. For $\mu>\mu_I$ the system resides in configuration II.

Configurations II and III are metastable in the regimes $\mu_{II}<\mu<\mu_I$ and $\mu_{III}<\mu<\mu_{II}$, respectively, and we expect hysteresis as μ is reduced from small negative values (thick films). This expectation is borne out experimentally.[3,7]

The discussion we have given here is somewhat different from the discussion given by Cole and Saam.[6] This is because Cole and Saam examined alternative configurations for a fixed number of particles, whereas we are choosing among configurations at the same chemical potential. Thus, they compared energies, whereas we compare grand potentials.

III. HYDRODYNAMIC MODES OF A SUPERFLUID ADSORBED ON NUCLEPORE

For the purpose of discussing the long-wavelength, low-frequency modes of a superfluid film adsorbed on Nuclepore we consider the system to be two dimensional. The superfluid is described by a complex order parameter, $\psi(\mathbf{r})$ which is a function of the position, $\mathbf{r}$, in the plane of the Nuclepore. The order parameter is taken to be coarse grained over cells which contain many pores, so that the number of pores in a cell can be replaced by the average number and the Nuclepore described by a homogeneous two-dimensional medium. The order parameter may be written in the form

$$\psi=\chi e^{i\phi} . \tag{3.1}$$

The superfluid areal density, $n(\mathbf{r})$, which includes superfluid in the pores and on the two surfaces, is given by

$$n(\mathbf{r})=[\chi(\mathbf{r})]^2 . \tag{3.2}$$

We assume that the coarse-grained order parameter $\psi(\mathbf{r})$ is related to a more microscopic order parameter which correctly describes the three-dimensional velocity field given by $(\hbar/m)$ times the gradient of the phase of this microscopic order parameter. In order to relate the microscopic phase to the coarse-grained phase we make the following two assumptions: First, the microscopic phase on the two surfaces is not significantly distorted by the presence of the pores so that, for long-wavelength disturbances, the superfluid velocity on the surfaces, $\mathbf{v}_s(\mathbf{r})$ is given by

$$\mathbf{v}_s(\mathbf{r})=(\hbar/m)\nabla\phi(\mathbf{r}) . \tag{3.3}$$

Secondly, we assume that the phase evolves linearly from one end of a pore to the other so that the superfluid velocity in a pore, $\mathbf{v}_p$ is given by

$$\mathbf{v}_p=[\mathbf{v}_s(\mathbf{r}_p)\cdot\hat{l}]\hat{l} , \tag{3.4}$$

where $\mathbf{r}_p$ is the position of the pore and $\hat{l}$ is a unit vector parallel to the axis of the pore. In Eq. (3.4) $\mathbf{v}_s$, $\mathbf{v}_p$, and $\hat{l}$ are three-dimensional vectors.

Both the equilibrium configuration of the superfluid and long-wavelength fluctuations about this equilibrium are determined by the time-dependent Landau-Ginzburg equation[8]

$$i\hbar\frac{\partial\psi(\mathbf{r})}{\partial t}=\frac{\delta\Omega[\psi;\mu]}{\delta\psi^*(\mathbf{r})} , \tag{3.5}$$

where $\Omega=E-\mu N$ is the grand potential functional for superfluid, the latter being in contact with a particle reservoir at chemical potential μ. For Ω, we take

$$\Omega[\psi;\mu]=\int d^2r\left[\frac{\hbar}{2m^*}|\nabla\psi|^2+e(|\psi|^2)-\mu|\psi|^2\right] , \tag{3.6}$$

where $e(n)$ is the internal energy density. The kinetic energy term can be split into two terms depending on the gradients of ϕ and χ, respectively. The former corresponds to the classical kinetic energy of the superfluid, while the latter is a quantum correction which is unimportant for long-wavelength phenomena and will be neglected hereafter. The effective mass, m^*, accounts for the fact that the fraction of fluid in the pores moves more slowly than $(\hbar/m)\nabla\phi$.

The effective mass can be calculated by equating the classical part of the kinetic energy in (3.6) to an expression determined by (3.3) and (3.4),

$$\tfrac{1}{2}\rho m(h+\lambda\Delta V/\alpha_T)\mathbf{v}_s^2=\frac{\hbar^2\chi^2}{2m^*}|\nabla\phi|^2 , \tag{3.7}$$

where ΔV is the volume of fluid in a pore, λ is the number of pores per unit area, and α_T is the tortuosity,[9] given by

$$\alpha_T^{-1}=\int d\hat{l}\, p(\hat{l})(\hat{l}\cdot\hat{\mathbf{k}})^2 . \tag{3.8}$$

$p(\hat{l})$ is the probability of finding a pore with direction $\hat{l}$, and $\hat{\mathbf{k}}$ is the direction of propagation of the disturbance.

From (3.7), we obtain

$$\frac{m^*}{m}=(\chi^2/\rho)(h+\lambda\Delta V/\alpha_T)^{-1}=n(n_s+n_p/\alpha_T)^{-1} , \tag{3.9}$$

where $n_s=\rho h$ and $n_p=\rho\lambda\Delta V$ are the superfluid areal density on the surfaces and in the pores, respectively.

The volume of fluid, ΔV_I, in a pore in configuration I is given by

$$\Delta V_I=\pi(2Rh_p-h_p^2)l , \tag{3.10}$$

while to a good approximation the volume of fluid, ΔV_{II}, in a pore in configuration II is just the volume of the pore itself,

$$\Delta V_{\rm II}=\pi R^2 l \ . \tag{3.11}$$

For a uniform distribution of pore directions with angles from the normal less than $\theta_{\max}=34°$, we have $\alpha_T=16$, independent of $\hat{\mathbf{k}}$.

The real and imaginary parts of (3.6) lead, respectively, to the continuity equation and a force law for the superfluid velocity. These can be combined in the usual way to form a wave equation with a propagation velocity, c, given by

$$c^2=\left[\frac{\partial^2 e}{\partial n^2}\right]\left[\frac{n}{m^*}\right]=\left[\frac{\partial\mu}{\partial n}\right]\left[\frac{n}{m^*}\right] . \tag{3.12}$$

This expression can be written in terms of the third- and fourth-sound velocities, c_3 and c_4,

$$\frac{1}{c_3^2}=\frac{m}{h}\frac{\partial h}{\partial\mu} \tag{3.13}$$

and

$$\frac{1}{c_4^2}=\frac{m}{\rho}\frac{\partial\rho}{\partial\mu} \ . \tag{3.14}$$

Combining (3.9) and (3.12) through (3.14), we obtain

$$\frac{1}{c^2}=(n_s+n_p/\alpha_T)^{-1}\left[\frac{n_s}{c_4^2}+\frac{n_s}{c_3^2}+\frac{n_p}{c_p^2}\right] , \tag{3.15}$$

where $c_p=c_4$ in configuration II, while in configuration I, c_p is given by

$$\frac{1}{c_p^2}=\frac{m}{\Delta V}\frac{\partial\Delta V}{\partial\mu} \tag{3.16}$$

and corresponds to the propagation speed of a surface mode of a film in the interior of a long tube of radius R.

For thin films, surface tension is unimportant, so that $c_p\simeq c_3$. Since n_s and n_p are comparable while $c_4\gg c_3$ and $\alpha_T\gg 1$, we have to good approximation, for thin films,

$$c=c_3(1+n_p/n_s)^{-1/2} \ . \tag{3.17}$$

As the film thickness increases, the fluid in the pore becomes elastically soft and $c_p\to 0$, so that near and below the transition ($\mu=\mu_{\rm I}$) the propagation speed approaches zero.

In configuration II, $c_p=c_4$, and $n_p\gg n_s$ while n_p/α_T and n_s are comparable so c may be greater than c_3 although less than c_4. Physically this corresponds to the fast propagation of the signal through the pores. The full behavior of (3.15) is shown in Fig. 4.

Our two-dimensional description of disturbances of the adsorbed film does not incorporate modes involving fluid motion in the direction perpendicular to the plane of the Nuclepore. There are in fact several such long-wavelength "optical" modes. One of these modes corresponds to out-of-phase height fluctuations of the fluid on the two surfaces of the Nuclepore. A second corresponds to the amount of fluid in the pores fluctuating out of phase with the height on the two surfaces. At long wavelengths and away from the instability in the pore, the characteristic frequencies of these modes correspond to sound velocities divided by the thickness of the Nuclepore and are thus of order 10^5 Hz or greater. These modes also approach zero frequency as the instability is approached and might be excited in the experiments of Ref. 3 very near the instability.

Within the context of a hydrodynamic description of a film in terms of the height h, and density ρ, there is also an optical mode with out-of-phase fluctuations of h and ρ. Such a mode would presumably have a long-wavelength frequency of order c_4/h. These modes should have no bearing on the low-frequency experiments described in Refs. 3 and 7.

IV. DISCUSSION

Experimental data has been obtained from Nuclepore filters with two different pore sizes, $R=10^{-5}$ cm and $R=4\times10^{-6}$ cm. For both pore sizes,[3,7] the data shows clearly three distinct regions, and the theoretical predictions are qualitatively in agreement throughout (see Fig. 4). For completeness, we include a plot, Fig. 5, of the predicted sound velocity as a function of h, showing the strong deviation from the h^{-3} dependence of third sound and the sharp transition to a fast mode propagating through the pores.

For low-^{4}He coverages, the sound velocity is much slower than that which would be found on a nonporous substrate, c^*, and the index of refraction, $\eta=c^*/c\simeq$constant>1. Physically, this is a consequence of the increased amount of fluid, ΔV, which must flow in

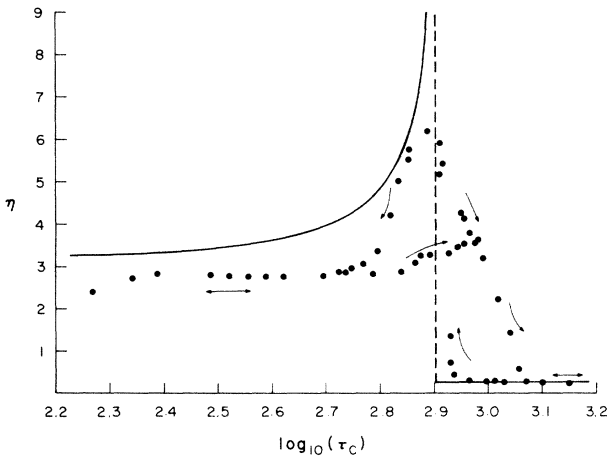

FIG. 4. Index of refraction. The index of refraction, η, is plotted versus $\log_{10}(\tau_c)$, with τ_c the time of flight on an otherwise identical but nonporous substrate. τ_c is in μsec, and the distance of travel is 0.635 cm as in Ref. 3 from which the data (solid points) has been taken. The solid line shows the theoretical prediction. Other parameters are as given in the text, except that $R=0.13$ μm has been used to account for a "barreling" effect in the interior of the pores (Ref. 1). The arrows show the direction in which the data was taken, and the dashed line marks the divergence in η at the instability of configuration I.

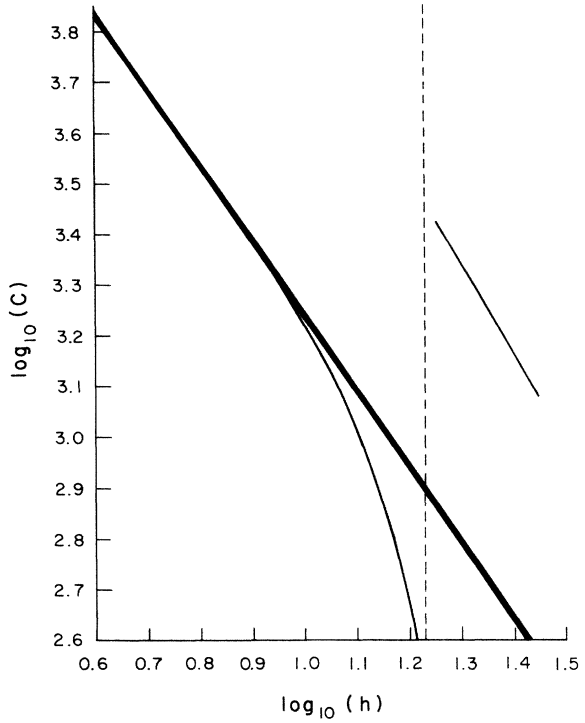

FIG. 5. Third sound velocity. The $\log_{10}$ of the third-sound velocity, c, is plotted as a function of $\log_{10}$ of the film thickness in layers, h. The thin solid line is the prediction for a porous substrate; the thick solid line is the prediction for a nonporous substrate. The dashed line marks the divergence in η at the instability in configuration I where $c \rightarrow 0$.

to and out of the pores as the wave passes. Since $h_p \simeq h$, $\partial V/\partial h$, and therefore η, is approximately constant. At high-^{4}He coverages, the pores are filled and $c_p = c_4 > c^*$. Thus, there is a fast mode with $\eta \simeq$ constant < 1 in this regime. For intermediate coverages, the experimental data shows a complicated hysteresis effect. This has been anticipated by our earlier discussion in that in this regime, two very different pore configurations may achieve equilibrium for the same surface ^{4}He thickness, h. We do not attempt to explain this phenomenon in detail, but only point out that the theory predicts a high peak for η in this regime, and this is indeed observed.

In an actual Nuclepore filter, there will be a range of pore sizes, as well as perhaps some complicated interior structure, such as the intersection of pores. Thus the peak in the data points in Fig. 4 should not necessarily be interpreted as the predicted instability of configuration I but may instead correspond to a metastable state of the system. Nonetheless, the qualitative agreement between theory and experiment establishes the value of our theoretical model in giving a simple physical picture and a computational scheme for understanding a complicated system.

ACKNOWLEDGMENTS

We would like to thank D. T. Smith, R. B. Hallock, and especially J. M. Valles for useful discussions, and for providing us with data prior to publication.

[1]Nuclepore Corp., Pleasanton, California.
[2]B. Bhattacharyya and F. M. Gasparini, Phys. Rev. Lett. **49**, 919 (1982).
[3]J. M. Valles, D. T. Smith, and R. B. Hallock, Phys. Rev. Lett. **54**, 1528 (1985).
[4]J. C. Noiray, D. Sornette, J. P. Romagnan, and J. P. Laheurte, Phys. Rev. Lett. **53**, 2421 (1984).
[5]B. Johnson, J. M. Valles, and R. B. Hallock (private communication).
[6]See also, e.g., W. F. Saam and M. W. Cole, Phys. Rev. B **11**, 1086 (1975); M. W. Cole and W. F. Saam, Phys. Rev. Lett. **32**, 985 (1974).
[7]D. T. Smith, J. M. Valles, and R. B. Hallock, Bull. Am. Phys. Soc. **30**, 712 (1985), and unpublished.
[8]R. A. Guyer (unpublished).
[9]T. J. Plona and D. L. Johnson, in *Physics and Chemistry of Porous Media,* edited by D. L. Johnson and P. N. Sen (AIP, New York, 1984), p. 89.